Dye-Sensitized Solar Cells: Sensitizer-Dependent Injection into ZnO Nanotube Electrodes

Rebecca A. Jensen, Hal Van Ryswyk,[†] Chunxing She, Jodi M. Szarko, Lin X. Chen, and Joseph T. Hupp*

Department of Chemistry, Northwestern University, 2145 Sheridan Road, Evanston, Illinois 60208.
[†] Current address: Department of Chemistry, Harvey Mudd College, 301 Platt Boulevard, Claremont, California 91711. vanryswyk@hmc.edu.

Two porphyrin-based dyes with carboxylic acid tethers of differing acidity in both protonated and deprotonated forms were examined on ZnO nanotube electrodes. All of the dyes have similar surface coverage, but only the more acidic dye in the acid form injects electrons well; this dye is the only one that corrodes the ZnO. In control experiments on TiO_2 nanoparticle electrodes, both dyes load and inject in protonated and deprotonated forms. These results are consistent with a requirement that the dye must partially corrode the ZnO surface in order for efficient injection to occur. Alternatively, it may possibly point to a coupling of electron injection to proton uptake.

Introduction

The overall efficiency of the best dye-sensitized solar cells (DSSCs) has been roughly 10% for the past 15 years.[1] Improving efficiency dramatically will require simultaneous changes in at least two, if not all three, of the critical components of the DSSC: dye, photoanode, and redox shuttle.[2] We are developing porphyrinic "superchromophores"[3] that absorb a wider fraction of the solar irradiance with peak extinction coefficients of more than an order of magnitude larger than those of extant optimized ruthenium-based dyes. We hope that, when combined with alternate photoanodes, these dyes will yield high efficiencies due to enhanced photocurrent densities and photovoltages. The photocurrent density is enhanced when the dye absorbs further into the red, capturing more of the solar spectrum. The photovoltage can be enhanced in two ways: (1) Higher-extinction dyes require fewer dye molecules and therefore a smaller effective photoanode surface area per unit geometric surface area to achieve high light-harvesting efficiencies. Thus, the dark-current density will decrease because the majority carrier interception by the redox couple is proportional to the electrode surface area. (2) A smaller effective photoanode surface area will ultimately allow faster redox shuttles with more positive redox potentials to regenerate the oxidized dye with a concomitant increase in photovoltage.

Moving to an oligomeric superchromophore requires a change in photoanode architecture.[2] Semiconductor nanotubes with a sufficiently gentle radius of curvature would allow efficient dye packing while providing aspect ratios large enough to achieve the necessary effective surface area. Motivated by the need for a better dye and a photoanode architecture optimized to its dimensions, we are developing prototype systems of porphyrin oligomers for use on ZnO,[4] TiO_2,[5] or SnO_2 nanotubes. Because ZnO is better than TiO_2 in terms of ease of fabrication on nanometer scales and its fast electron-transport property,[6] we use ZnO nanotubes to screen a range of porphyrin monomers.

In this letter, we report the discovery that the nature of the porphyrin dye's tethering group greatly affects electron injection efficiency on ZnO nanotubes. Acidic tethering groups that corrode ZnO nanotubes result in surprisingly improved electron injection efficiency and thus improved overall cell efficiency. Deprotonated tethering groups lead to poor injection efficiency and low overall cell efficiency. In control experiments, this tether dependence is not seen with TiO_2 nanoparticle photoanodes.

Experimental Methods

Porphyrin dyes were synthesized as detailed in the Supporting Information. N719 dye or $[Bu_4N]_2(Ru(mpdcbpy)_2(SCN)_2)$, where mpdcbpy is monoprotonated 4,4′-dicarboxy-2,2′-bipyridine, was used as received from DyeSol.

ZnO nanotube photoanodes were created on anodized aluminum oxide (AAO) substrates.[5] The 60-μm-thick AAO is penetrated by 200-nm-diameter pores that traverse the AAO, narrowing to 20 nm diameter within 2 μm of the base. The pores were conformally coated with 11 nm of ZnO via atomic layer deposition (ALD). In a departure from earlier work, an additional 24 nm of ZnO was deposited using nonconformal ALD conditions across the base of the AAO to occlude the 20-nm-diameter pores. The electrodes were fired at 450 °C for 30 min.

*Corresponding author. E-mail: j-hupp@northwestern.edu.

(1) (a) Gratzel, M.; Kalyanasundaram, K. *Curr. Sci.* **1994**, *66*, 706–14. (b) Chiba, Y.; Islam, A.; Komiya, R.; Koide, N.; Han, L. Y. *Appl. Phys. Lett.* **2006**, 88. (c) Chiba, Y.; Islam, A.; Watanabe, Y.; Komiya, R.; Koide, N.; Han, L. Y. *Jpn. J. Appl. Phys., Part 2* **2006**, *45*, L638–L640. (d) Gratzel, M. *Inorg. Chem.* **2005**, *44*, 6841–6851. (e) Gratzel, M. *MRS Bull.* **2005**, *30*, 23–27. (f) Kroon, J. M.; Bakker, N. J.; Smit, H. J. P.; Liska, P.; Thampi, K. R.; Wang, P.; Zakeeruddin, S. M.; Gratzel, M.; Hinsch, A.; Hore, S.; Wurfel, U.; Sastrawan, R.; Durrant, J. R.; Palomares, E.; Pettersson, H.; Gruszecki, T.; Walter, J.; Skupien, K.; Tulloch, G. E. *Prog. Photovoltaics* **2007**, *15*, 1–18. (g) Nazeeruddin, M. K.; DeAngelis, F.; Fantacci, S.; Selloni, A.; Viscardi, G.; Liska, P.; Ito, S.; Takeru, B.; Gratzel, M. *J. Am. Chem. Soc.* **2005**, *127*, 16835–16847. (h) Wang, Z.-S.; Yanagida, M.; Sayama, K.; Sugihara, H. *Chem. Mater.* **2006**, *18*, 2912–2916. (i) Wei, M. D.; Konishi, Y.; Zhou, H. S.; Yanagida, M.; Sugihara, H.; Arakawa, H. *J. Mater. Chem.* **2006**, 16.

(2) Hamann, T. W.; Jensen, R. A.; Martinson, A. B. F.; Van Ryswyk, H.; Hupp, J. T. *Energy Environ. Sci.* **2008**, *1*, 66–78.

(3) (a) Anderson, H. L. *Chem. Commun.* **1999**, 2323–2330. (b) Kumble, R.; Palese, S.; Lin, V. S. Y.; Therien, M. J.; Hochstrasser, R. M. *J. Am. Chem. Soc.* **1998**, *120*, 11489–11498.

(4) Martinson, A. B. F.; Elam, J. W.; Liu, J.; Hupp, J. T.; Pellin, M. J.; Marks, T. J. *Nano Lett.* **2008**, *8*, 2862–2866.

(5) Martinson, A. B. F.; Elam, J. W.; Hupp, J. T.; Pellin, M. J. *Nano Lett.* **2007**, *7*, 2183–2187.

(6) (a) Zhang, Q. F.; Dandeneau, C. S.; Zhou, X. Y.; Cao, G. Z. *Adv. Mater.* **2009**, 1–22. (b) Ozgur, U.; Alivov, Y. I.; Liu, C.; Teke, A.; Reshchikov, M. A.; Dogan, S.; Avrutin, V.; Cho, S. J.; Morkoc, H. *J. Appl. Phys.* **2005**, *98*, 041301−1–041301−103.

Table 1. Dye Loading and Photovoltaic Performance of ZnO- and TiO$_2$-Based DSSCs Using Porphyrins of Differing Acidity as Sensitizers versus N719 Controls

dye /semiconductor	dye loading^a	J_{sc}/mA cm^{-2}	V_{oc} /mV	ff	η/%
1a/ZnO	130	0.11	340	0.56	0.02
1b/ZnO	390	0.07	290	0.54	0.01
2a/ZnO	390	1.3	500	0.66	0.5
2b/ZnO	390	0.34	400	0.7	0.1
N719/ZnO	390	2.7	680	0.59	1.1
1b/TiO$_2$	1100	5.9	650	0.66	2.5
2a/TiO$_2$	1100	6.2	620	0.59	2.3
N719/TiO$_2$	1100	7.7	730	0.63	3.5

^{a} The enhanced number of molecules adsorbed on a porous surface relative to the number adsorbed on a flat surface as measured by dye desorption.

Electrical contact was established across the occluded base by sputtering 50 nm of silver. These photoanodes were illuminated through the electrolyte by light incident on the translucent Pt/fluorine-doped tin oxide counter electrode.

Nanocrystalline 8-μm-thick TiO$_2$ photoanodes were prepared from 20-nm-diameter TiO$_2$ anatase particles (DyeSol) atop 10-nm-thick TiO$_2$ ALD layers on fluorine-doped tin oxide plates. The films were sintered at 500 °C for 30 min. These cells were illuminated through the photoanode.

Porphyrin dyes were deposited on ZnO-coated AAO from 1 mM solutions in THF for 20 min to 8 h to test the corrosion effect on cell performance. For **2a**/ZnO cells with deposition times of less than 2 h, no corrosion or significant change in cell performance is observed. Thus, all porphyrin dye cells reported here were deposited for 20 min on ZnO-coated AAO and for 8 h on TiO$_2$ photoanodes. (No acid corrosion is observed on TiO$_2$.) N719 was deposited from 0.1 mM solutions in ethanol for 20 min on ZnO-coated AAO and for 8 h on TiO$_2$ substrates. The loading of porphyrin dyes was expressed as the ratio of the effective occupied surface area over the geometrical area by measuring desorbed dyes (in 0.1 M KOH in methanol) relative to the theoretical number of molecules on a flat surface, thus reflecting the enhanced number of molecules adsorbed on photoanodes (column 2 of Table 1). The electrolyte for photoelectrochemical measurements consisted of 0.6 M butylmethylimidazolium iodide, 0.05 M I$_2$, 0.1 M LiI, and 0.5 M *tert*-butyl pyridine in 1:1 acetonitrile/valeronitrile.

Cells were illuminated through an Oriel 81092 filter at 98 mW cm^{-2} using a Xe lamp. Fluorescence was measured using a Fluorolog-3 (Jobin Yvon). A CH Instruments 1200A potentiostat was used to record current–voltage curves.

Transient absorption (TA) measurements were performed using a Coherent RegA 9050 regenerative amplifier operating at a repetition rate of 150 kHz and providing 50 fs fwhm pulses of 800 nm. Roughly 50% of the output was used to generate second-harmonic 400 nm photons, which were used for pump excitation. Another 25% of the light was passed through a sapphire window to create a white-light continuum. TA measurements were made on dye/ZnO films on glass without electrolyte.

Results and Discussion

System. ZnO nanotubes produced by ALD on commercially available AAO supports are an easy-to-fabricate photoanode for the preliminary screening of dyes. The nanotubes employed here can be constructed on commercially available ALD equipment in two steps and have a roughness factor of 400 times the geometric area.[5] These cells are prototypes for the rapid screening of dye loading and injection efficiencies and are not designed to maximize overall conversion efficiency. For example, there is considerable loss in photon flux (roughly 20%) associated with backside illumination through the Pt-coated conductive oxide counter electrode in these test cells. In a similar vein, light
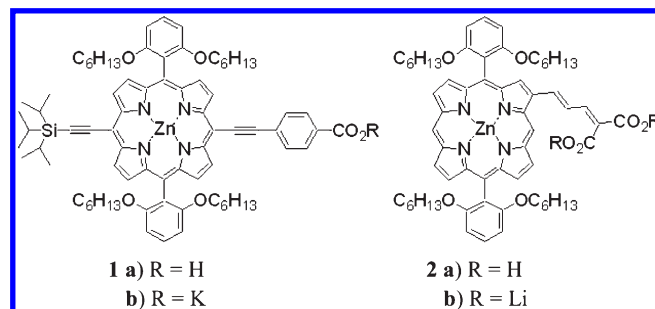
Figure 1. Porphyrin dyes.
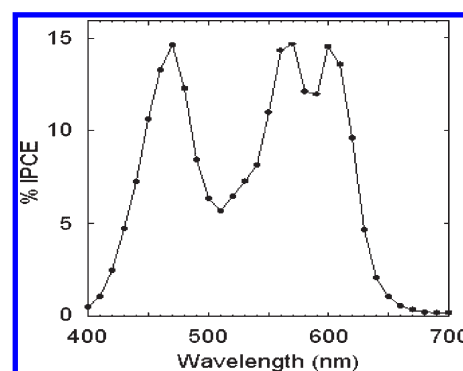
Figure 2. IPCE measured over 10 nm intervals for **2a** on 60-μm-thick ZnO nanotube photoanodes. The dye deposition time is 20 min.

scattering off of the AAO support further decreases the conversion efficiency. Both of these limitations could be surmounted in a next-generation design aimed at maximizing the conversion efficiency.

The *meso*- and *beta*-tethered porphyrin dyes are shown in Figure 1. The substituted aryl groups in both dyes simultaneously serve to increase the overall dye solubility in THF and to suppress aggregation upon adsorption. These porphyrin dyes strongly absorb in their Soret and Q bands at ~470 and ~600 nm, respectively (Figure S1).

Porphyrins on ZnO Nanotubes. Dyes **1b**, **2a**, and **2b** load equally well onto ZnO nanotube structures, but **1a** does not load as well (Table 1). Of these dyes, only **2a** produces significant photocurrents (> 1 mA cm^{-2}); the next best porphyrin dye (**2b**) produces photocurrents that are 4-fold lower. Excitation into the porphyrin Q bands at 560 and 600 nm yields an incident photon-to-current efficiency (IPCE) equal to that obtained by exciting the more strongly absorbing Soret band at 470 nm (Figure 2). Even though the light-harvesting efficiencies for the Q bands are lower than that of the Soret band, it is known that photogenerated electrons can be collected throughout the full 60 μm depth of the ZnO nanotube.[7] For comparison, IPCE for widely studied ruthenium dye N719 on these ZnO nanotubes (not shown) reaches a maximum of 20% at 535 nm. The lower-maximum IPCE of **2a** relative to that of N719 likely reflects a combination of lower injection efficiency (due in part to quenching of the dye excited state by triiodide[8]) and increased charge interception by triiodide (due to a higher concentration of triiodide at the semiconductor surface through association with the porphyrin dye). Organic dyes are known to catalyze interception when

(7) Martinson, A. B. F.; Goes, M. S.; Fabregat-Santiago, F.; Bisquert, J.; Pellin, M. J.; Hupp, J. T. *J. Phys. Chem. A* **2009**, *113*, 4015–4021.
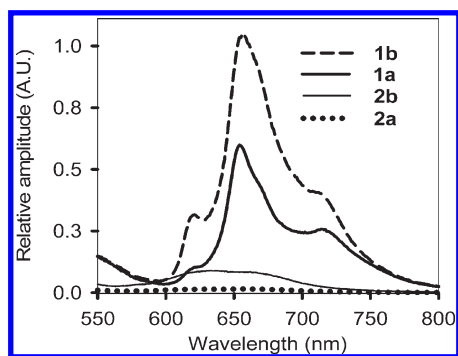(8) Splan, K. E.; Massari, A. M.; Hupp, J. T. *J. Phys. Chem. B* **2004**, *108*, 4111–4115.

Figure 3. Emission spectra of porphyrin dyes **1a**, **1b**, **2a**, and **2b** on ZnO nanotubes with 430 nm excitation in the absence of electrolyte. Emission intensities are corrected to correspond to the same dye absorbance at 430 nm.

paired with triiodide electrolyte; this effect suppresses the open-circuit photovoltage.[8,9]

Efficient electron injection in **2a**/ZnO is suggested by comparing the emission spectra of the four porphyrin dyes on ZnO nanotubes with no electrolyte present to avoid strong scattering and/or absorption by the Pt electrode and FTO (Figure 3). The dye fluorescence intensity on ZnO decreases in the order **1b** > **1a** > **2b** > **2a**, whereas the fluorescence intensity of the same dyes on bare AAO is largely invariant (not shown). The lack of fluorescence quenching on the alumina surface is indicative of the absence of a viable charge-injection pathway on this substrate, and the quenching behavior on ZnO is indicative of increasing charge injection into ZnO across this series of dyes, matching the pattern of increasing current densities observed in the ZnO cells (Table 1).

Electron injection dynamics were directly measured by monitoring the excited-state decay at 800 nm using ultrafast TA spectroscopy since the excited states of the porphyrin dyes absorb in the near-IR region (Figure S2). Figure 4 compares excited-state decays (in the first 100 ps) for **2a** in toluene and **2a**, **2b**, and **1a** on ZnO nanotubes excited at 400 nm.[10] The excited states of all of the dyes decay within 1 to 2 ns, which is defined as τ_0, as can be seen for **2a** in fluorescence upconversion measurements in toluene (Figure S3). Without quenching due to electron injection, the excited state of **2a** in toluene barely decays in 100 ps. However, an additional accelerated component, τ_{fast}, of the excited-state decay is observed in the order **2a** > **2b** > **1a** on ZnO when they undergo electron injection. From the relationship $1/\tau_{inj} = 1/\tau_{fast} - 1/\tau_0$, the relative electron injection rates are in the same order. Thus the injection time (τ_{inj}) for **2a**/ZnO is roughly 11 ps, and the injection time for **2b** is roughly 35 ps. Because TA measurements were made on dye/ZnO substrates on glass (not in assembled cells with FTO and electrolyte), the absolute injection times might be different from those in assembled cells. However, the trend in electron injection rates corroborates the observation of different current densities (Table 1).

The loading of **2a** from a 1 mM solution in THF on ZnO nanotubes is invariant with time between 20 min and 2 h.
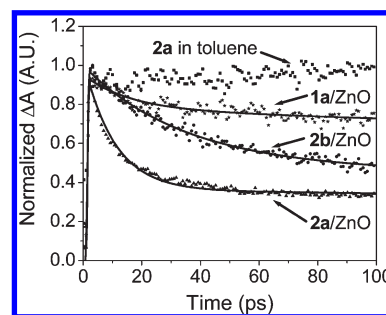
(9) (a) O'Regan, B. C.; Lopez-Duarte, I.; Victoria Martinez-Diaz, M.; Forneli, A.; Albero, J.; Morandeira, A.; Palomares, E.; Torres, T.; Durrant, J. R. *J. Am. Chem. Soc.* **2008**, *130*, 2906–2907. (b) Miyashita, M.; Sunahara, K.; Nishikawa, T.; Uemura, Y.; Koumura, N.; Hara, K.; Mori, A.; Abe, T.; Suzuki, E.; Mori, S. *J. Am. Chem. Soc.* **2008**, *130*, 17874–17881.

(10) Electrons in the conduction band also absorb at 800 nm, with a much smaller extinction coefficient than that of the dye excited state. Electron absorption does not contribute significantly to the observed dynamics because the dynamics of electron absorption increases with time. The data of **1b** is not shown as a result of a poor signal-to-noise ratio and strong sample scattering.

Figure 4. Excited-state decay for **2a**, **2b**, and **1a** on ZnO nanotubes and **2a** in toluene monitored at 800 nm. Dots are experimental data, and solid lines are fits. Excitation is at 400 nm.

A noticeable fogging of the photoanode due to the corrosion of ZnO is observed after 2 h; after 4 h, the photoanode is opaque. Similar behavior is observed with N719, whereas none of the other porphyrin dyes are observed to corrode the ZnO. Attempts to visualize corrosion on the 11-nm-thick nanocrystalline ZnO nanotube walls with **2a** via scanning electron microscopy over short deposition times (< 2 h) were inconclusive. In the range of 2–4 h, a thinning of the walls is evident. After 4 h, gaps appear in the tube walls.

The tendency of N719 and its fully protonated, more acidic analogue N3 to corrode ZnO to form Zn^{2+}/dye aggregates is well established;[11] for this reason, adsorption times for 0.1 mM N719 in ethanol on ZnO are typically limited to less than 30 min. Dyes **1a** and **2a** have estimated pK_a values of 4.0 and 2.4,[12] respectively, whereas the pK_a values for N3 have been measured to be 1.5 and 3.0 for two successive proton equilibria.[13] Assuming that the pK_a of N719 and the second pK_a of N3 are roughly equivalent, the advent of corrosion of the ZnO/AAO films occurs with dyes with pK_a values between 3 and 4.

In summary, of all of the dyes examined on ZnO, both porphyrinic and ruthenium-based, only those in the acid form with a pK_a < 4 corrode ZnO and inject efficiently.

Comparison with TiO$_2$ Nanoparticles. Cells assembled from dyes adsorbed on 8 μm thick TiO$_2$ nanoparticle photoanodes provide additional information on dye injection efficiencies. Both dyes **1b** and **2a** on TiO$_2$ nanoparticles yield essentially identical efficiencies of ca. 2.4% (Table 1). Thus **1b** is a viable dye on TiO$_2$, but not on ZnO. Dye desorption measurements show the surface coverage to be similar, with overall loading analogous to that of N719. The IPCEs track the absorbance spectra of the dyes, with **1** showing red-enhanced Q bands due to the asymmetric pattern of extended conjugation present in the porphyrin structure (Figure 5). IPCE tops out at roughly 40% for the porphyrin Soret bands, with lower values for the Q bands. For comparison, the IPCE for N719 (not shown) approaches 50% in these nonoptimized cells that do not employ scattering layers. The 8-μm-thick photoanodes are nearly opaque when loaded with porphyrins: the light-harvesting efficiency exceeds 0.75 for the Soret and Q bands. The decrease in IPCE in the Q bands relative to the Soret bands suggests a difference in injection efficiency in this configuration. This decrease in IPCE with band as well as the slightly lower maximum IPCE relative to N719 is symptomatic of the lower sensitizing efficiency of the porphyrin dyes. The lower porphyrin photovoltages relative to N719 on TiO$_2$ correlate with

(11) Horiuchi, H.; Katoh, R.; Hara, K.; Yanagida, M.; Shigeo, Murata; Arakawa, H.; Tachiya, M. *J. Phys. Chem. B* **2003**, *107*, 2570–2574.

(12) Adv. Chem. Dev. Lab., 2008.

(13) Nazeeruddin, M. K.; Zakeeruddin, S. M.; Humphry-Baker, R.; Jirousek, M.; Liska, P.; Vlachopoulos, N.; Shklover, V.; Fischer, C. H.; Gratzel, M. *Inorg. Chem.* **1999**, *38*, 6298–6305.
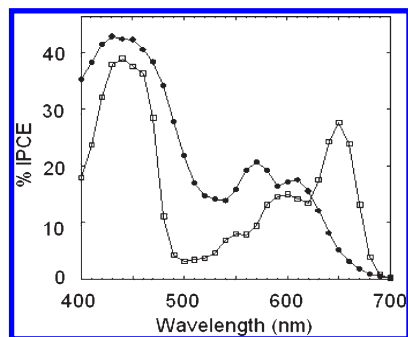
Figure 5. IPCE measured over 10 nm intervals for **1b** (□) and **2a** (●) on 8-μm-thick TiO$_2$ nanoparticle photoanodes.

the much larger dark currents observed for the porphyrins (not shown). Acid **1a** does not load as effectively as potassium salt **1b**. The reasons for this loading disparity on TiO$_2$ are unclear but may be solubility-related. Although there is ample precedent for overall efficiencies varying with the carboxylate counterion,[14] the efficiency obtained with potassium salt-based **1b** in this configuration is notable for its high value relative to its acid form.

The lower IPCE at any given wavelength for the ZnO cells (Figure 2) relative to the that of the corresponding TiO$_2$ cells (Figure 5) is ascribed to three effects: (1) the smaller amount of dye present in the nanotube photoanodes because of the smaller roughness factor; (2) the fraction of light lost through scattering by the AAO; and (3) reflective and absorption losses associated with illumination through the counter electrode and electrolyte in this simple AAO-supported configuration.

Dye/Photoanode Interactions. The most striking difference in the behaviors of the porphyrin dyes in ZnO- and TiO$_2$-based cells is the inability of **1b** to inject efficiently into the ZnO devices. The two dyes that inject efficiently into ZnO, **2a** and N719, share the ability to corrode ZnO at long deposition times. This corrosive ability correlates with the pK_a of the acid tether.

A recent study using single-crystal ZnO in aqueous electrolyte demonstrated that the dissolution of the oxide surface starts at pH 5.5 and occurs selectively at pre-existing step edges, which consist of nonpolar surfaces. In comparison, oxide dissolution along the ZnO(0001) direction proved to be effectively inhibited above a pH of 3.8.[15] All of this occurs at pH values well below the point of zero charge for ZnO, which is 8.7. While our polycrystalline

11-nm-thick films (nanotubes) in THF or ethanol are clearly different from a single-crystal ZnO system in aqueous electrolyte, the empirical correlation of film stability with dye acid strength suggests that effective adsorption and subsequent electron injection may require a preliminary, dye-based corrosion of the ZnO substrate.

There are alternative explanations. For example, a pH-dependent photocurrent has been observed for porphyrin dyes on TiO$_2$ films in aqueous electrolyte.[16] This effect was attributed to a pH-dependent charge collection efficiency wherein the protonation of a surface site is required for the effective charge compensation of injected electrons.[17] The magnitude of the sensitized photocurrent is determined by surface protonation−deprotonation equilibria. Additional work supports the charge-compensation-based adsorption/intercalation phenomenon playing a key role in defining the conduction band edge energetics of titanium dioxide[18] and other metal oxides[19] in solution environments.

Conclusions

Porphyrin and ruthenium dyes with pK_a ≤3 have been shown to corrode thin films of ZnO produced via ALD in a nanotube architecture. These dyes inject efficiently, whereas porphyrin dyes with pK_a >3 may load to a similar extent and inject on nanoparticulate TiO$_2$ but do not inject on ZnO. We surmise that in order for efficient electron injection into ZnO films to occur the films must (a) be partially corroded by the dye and/or (b) couple the injection to interfacial proton adsorption or intercalation.

Supporting Information Available: Synthetic details, UV−vis absorption spectra of porphyrin dye cells, and TA and fluorescence upconversion measurements of **2a** in toluene. This material is available free of charge via the Internet at http://pubs.acs.org.

(14) Campbell, W. M. *Coord. Chem. Rev.* **2004**, *248*, 1363–1379.

(15) Valtiner, M.; Borodin, S.; Grundmeier, G. *Langmuir* **2008**, *24*, 5350–5358.

(16) Watson, D. F.; Marton, A.; Stux, A. M.; Meyer, G. J. *J. Phys. Chem. B* **2004**, *108*, 11680–11688.

(17) Staniszewski, A.; Ardo, S.; Sun, Y.; Castellano, F. N.; Meyer, G. J. *J. Am. Chem. Soc.* **2008**, *130*, 11586–11587.

(18) (a) Lyon, L. A.; Hupp, J. T. *J. Phys. Chem.* **1995**, *99*, 15718–15720. (b) Lyon, L. A.; Hupp, J. T. *J. Phys. Chem. B* **1999**, *103*, 4623–4628. (c) Lemon, B. I.; Hupp, J. T. *J. Phys. Chem.* **1996**, *100*, 14578–14580.

(19) (a) Lemon, B. I.; Hupp, J. T. *J. Phys. Chem. B.* **1997**, *101*, 2426–2429. (b) Lemon, B. I.; Liu, F.; Hupp, J. T. *Coord. Chem. Rev.* **2004**, *248*, 1225–1230.